THE JOURNAL OF BIOLOGICAL CHEMISTRY
Vol. 279, No. 8, Issue of February 20, pp. 7091–7097, 2004
Printed in U.S.A.

Histone Acetyltransferase-dependent Chromatin Remodeling and the Vascular Clock*

Received for publication, October 31, 2003, and in revised form, November 24, 2003
Published, JBC Papers in Press, November 26, 2003, DOI 10.1074/jbc.M311973200

Anne M. Curtis‡, Sang-beom Seo§¶, Elizabeth J. Westgate‡, Radu Daniel Rudic‡, Emer M. Smyth‡, Debabrata Chakravarti¶, Garret A. FitzGerald‡¶‖, and Peter McNamara‡**

*From the ‡Center for Experimental Therapeutics and ¶Department of Pharmacology, University of Pennsylvania, Philadelphia, Pennsylvania 19104, the §College of Dentistry, Seoul National University, 28 Yeongun-dong, Chongno-gu, Seoul, Korea, and the **Phenomix Corporation, La Jolla, California 92037*

Rhythmic gene expression is central to the circadian control of physiology in mammals. Transcriptional activation of Per and Cry genes by heterodimeric bHLH-PAS proteins is a key event in the feedback loop that drives rhythmicity; however, the mechanism is not clearly understood. Here we show the transcriptional coactivators and histone acetyltransferases, p300/CBP, PCAF, and ACTR associate with the bHLH-PAS proteins, CLOCK and NPAS2, to regulate positively clock gene expression. Furthermore, Cry2 mediated repression of NPAS2:BMAL1 is overcome by overexpression of p300 in transactivation assays. Accordingly, p300 exhibits a circadian time-dependent association with NPAS2 in the vasculature, which precedes peak expression of target genes. In addition, a rhythm in core histone H3 acetylation on the *mPer1* promoter *in vivo* correlates with the cyclical expression of their mRNAs. Temporal coactivator recruitment and HAT-dependent chromatin remodeling on the promoter of clock controlled genes in the vasculature permits the mammalian clock to orchestrate circadian gene expression.

Circadian rhythms, which are generated by cell autonomous biological clocks, allow for the appropriate temporal synchronization of physiology and behavior, optimizing the efficiency of biological systems (1, 2). In mammals, the circadian timing system is hierarchical, with the master clock located in the hypothalamic suprachiasmatic nuclei (SCN)[1] (3). Circadian oscillators have been uncovered in both central and peripheral tissues, with the suprachiasmatic nucleus (SCN) coordinating temporal physiology by synchronizing peripheral oscillators through both neural and humoral outputs (4–8).

Transcriptional regulation is central to clock function. Pacemaker rhythms are generated and sustained by positive and negative transcriptional/translational feedback loops (9). Positive components include the bHLH-PAS proteins CLOCK and BMAL1 (also known as MOP3) driving transcription as functional heterodimers through E-box enhancer elements (CACGTG) (10). NPAS2 (also known as MOP4) is a paralogue of CLOCK and behaves similarly in cell and biochemical assays (8, 11–14). We have observed a robust rhythm in NPAS2 mRNA expression in the aorta, kidney, and heart. Furthermore, NPAS2 can operate in the core feedback loop in the vasculature and forebrain (8, 13, 14). Known targets for these effector molecules are the Period (*Per1-3*) and Cryptochrome (*Cry1-2*) genes (2). As PER and CRY cytoplasmic levels rise, they can translocate back to the nucleus, and negatively regulate their own transcription by directly interacting with CLOCK:BMAL1 or NPAS2:BMAL1 heterodimers (9, 15). Thereafter, nuclear levels of the PER/CRY complex decline, relieving repression on the bHLH-PAS heterodimer and restarting the cycle with a period of ~24 h. The positive limb of the feedback loop also involves the regulation of *bmal1*, which cycles robustly antiphase to *Per* and *Cry* (9). CLOCK and BMAL1 also drive the expression of the orphan nuclear receptor *Rev-erbα* in the SCN and liver (16). The *Bmal1* gene contains Rev-Erbα/ROR response elements in its promoter, and its expression is repressed by Rev-Erbα (16). Therefore as *Per*, *Cry*, and *Rev-erbα* levels rise, *Bmal1* levels fall. The precise regulation of circadian timing systems extends beyond RNA kinetics and includes recently identified transcriptional and post translational modifications (17, 18). For example, CLOCK, BMAL1, PER1, and PER2 all undergo temporal changes in phosphorylation in mouse liver. These affect their activity, stability, and subcellular localization (18, 19)

Covalent modifications of histones on the chromatin template, such as acetylation, phosphorylation, and methylation, influence gene specific regulation (20). The correlation between acetylation of core histones and transcriptional induction has been well established (21, 22). The association of transcription factors, recruitment of coactivator complexes, and the targeting of gene promoters to induce histone acetylation and chromatin remodeling is a sequential process, resulting in transcriptional activation. Indeed, CREB-binding protein (CBP) is known to associate directly with RNA polymerase II (23) a critical step in the rapid assembly of functional preinitiation complexes at promoters (24, 25). For example, p300/CBP-associated factor (PCAF) preferentially acetylate histone H3, while histone H3 and histone H4, are substrates for p300/CBP. Previous reports, linking light exposure during subjective day to histone H3 phosphorylation and associated SCN induction of circadian genes, strongly suggests that chromatin remodeling complexes might temporally regulate rhythmic gene expression exhibited by clock genes in the circadian feedback loop (26). Furthermore, Etchegaray *et al.* (27) recently demonstrated an important role for histone acetylation in regulating circadian gene expression. These studies examined the role of CLOCK: p300-dependent

* This work was supported in part by Grants HL-54500, DK 57079 (to D. C.), and HL-62250 from the National Institutes of Health. The costs of publication of this article were defrayed in part by the payment of page charges. This article must therefore be hereby marked "*advertisement*" in accordance with 18 U.S.C. Section 1734 solely to indicate this fact.

‖ The Robinette Foundation Professor of Cardiovascular Medicine. To whom correspondence should be addressed. Tel.: 215-898-1185; Fax: 215-573-9135; E-mail: garret@spirit.gcrc.upenn.edu.

[1] The abbreviations used are: SCN, suprachiasmatic nucleus; CBP, CREB-binding protein; PCAF, p300/CBP-associated factor; RNA Pol II, RNA polymerase II; ChIP, chromatin immunoprecipitation; HAT, histone acetyltransferase; Per, Period; Cry, Cryptochrome; HVSMC, human vascular smooth cells.

chromatin remodeling in the liver. We report that this mechanism extends to a distinct peripheral clock in the vasculature where it involves a CLOCK paralogue, NPAS2 and modulates Cry-dependent repression of cyclical gene expression.

EXPERIMENTAL PROCEDURES

Cell Culture—HeLa 229 cells were grown to ~70% confluence and serum shock with 50% fetal bovine serum was carried out as described (8). Cells were harvested at indicated post-serum induction time points.

Animal Handling and Tissue Harvesting—8–12-week-old c57Bl/6 wild-type male mice were synchronized to a 12:12 light/dark cycle for a period of 2 weeks before placing in DD. The animals were anesthetized at indicated time intervals and then exsanguinated. Tissues were harvested, immediately flash-frozen in liquid nitrogen and stored at −70 °C.

Chromatin Immunoprecipitation Assay—Chromatin immunoprecipitations (ChIP) were carried out on HeLa cells using the ChIP assay kit (Upstate Biotechnology). ChIP assays were performed on mouse tissue as described (28–30) with slight modifications. Cells were resuspended in lysis buffer containing protease inhibitors and sonicated using a Misonix Sonicator 3000 for four 15-s bursts at setting 4 for cells or eight 40-s bursts at setting 4 for tissue: this results in DNA being fragmented to sizes of 500–1000 base pairs. Immunoprecipitations were carried out using a range of antibodies: anti-acetyl Histone 3 (acetylated lysine residues 9, 14, 18, and 23), anti-acetyl Histone 4 (acetylated lysine residues 5, 8, 12, and 16) from Upstate Biotechnology and anti-Pol II (Santa Cruz Biotechnology), which recognizes the N terminus of the large subunit of human RNA polymerase II. ChIP assays were also performed in the absence of antibody or the presence of anti-hemagglutinin (Santa Cruz Biotechnology) to control for nonspecific interactions. Immunoprecipitated DNA was analyzed by real-time PCR (ABI Prism 7000, PE Applied Biosystems).

RNA Analysis—Total RNA was extracted from cells and mouse heart tissue using RNAqueous (Ambion) and TRIzol (Invitrogen). RNA (400 ng) was used in a reverse transcription (RT) reaction (Applied Biosystems Reverse Transcription Kit). The resulting cDNA (40 ng) for each time interval was subjected to quantitative Real Time PCR.

Quantitative Real Time PCR—Primers for RNA and ChIP analysis were designed by PRIMER EXPRESS 1.0 (PE Applied Biosystems) to amplify 50–150-bp amplicons and the DNA intercalating SyBr green reagent (Applied Biosystems) was used for detection of all products. The relative differences among the intervals following serum induction for ChIP and RNA expression were calculated using the $\Delta\Delta C_T$ method as described (Applied Biosystems User Bulletin 2). A ΔC_T value was calculated for GAPDH to account for differences in starting material for RNA expression and a ΔC_T for the ChIP total input control to normalize for variation in the amount of starting material. Primer sequences: hPer 1 promoter, 5′-CTTCAATTGTCCGCATCCTT-3′ and 3′-TCAAATCCTGGGAGAGGACAGT-5′; mPer1 promoter, 5′-GCTGACTGAGCGGTGTCTGA-3′ and 3′-AAGGATCTCTTCCTGGCATCTG-5′; hPer1, 5′-TCCATTCGGGTTACGAAGCT-3′ and 3′-GCAGCCCTTTCATCCACATC-5′; hPer2, 5′-AGGGTGCGCTCGTTTGAA-3′ and 3′-GGCGGAAATTCCGCGTAT-5′; mPer1, 5′-TCGAAACCAGGACACCTTCTCT-3′ and 3′-GGGCACCCCGAAACACA-5′; mPer2, 5′- GCTCGCCATCCACAAGAAG-3′ and 3′-GCGGAATCGAATGGGAGAATA-5′; mClock, 5′-CGGCGAGAACTTGGCATT-3′ and 3′-AGGAGTTGGGCTGTGATCA-5′; mNpas2, 5′-TCCATGCTCCCTGGTAACACT-3′ and 3′- TCTGCAAGAATCCGATGACCTT-5′; mBmal1, 5′-CACTGTCCCAGGCATTCCA-3′ and 3′-TTCCTCCGCGATCATTCG-5′; mCry2 5′-CCATTATGAAGATGGCCAAGGA-3′ and 3′- CTGCCCATTCAGTTCGATGATT-5′; Rev-erba 5′-CCGGACTGTGCAGGAGATCT-3′ and 3′- CACCTGGTCGTGCTGAGAAAG-5′.

In Vitro Interaction Assays—^{35}[S]methionine-labeled BMAL1, CLOCK, NPAS2, ACTR, CBP, p300, and PCAF were synthesized by Promega (TNT-coupled Reticulocyte Lysate Systems), run on SDS-PAGE gel, and expression analyzed by phosphorimager. ^{35}[S]methionine-labeled BMAL1, CLOCK, and NPAS2 were incubated with recombinant FLAG-tagged p300 and PCAF, and immunoprecipitated with or without anti-p300 and anti-PCAF antibodies (Santa Cruz Biotechnology) or with Rabbit IgG as a control for co-immunoprecipitation assays. GST-NPAS2 was synthesized using the pGEX4T vector (Amersham Biosciences) and used in GST pull-down assays as described (8, 31). GST alone and GST-NPAS2 were run on a 12% Coomassie-stained SDS gel, and equal amounts were determined for pull-down experiments. Equal amounts of GST-NPAS2 and GST were incubated with ^{35}[S]methionine-labeled ACTR, CBP, p300, and PCAF for 2 h at 4 °C. The beads were washed extensively and analyzed by phosphorimager.

CBP and NPAS2 were subcloned into the GAL4DBD and VP16 vectors respectively for cell-based assays. CV-1 cells were transfected with the pMH100TKLuc reporter along with combinations of GAL4, GAL4NPAS2, VP16, and VP16CBP. Cells were harvested 48 h post-transfection and assayed for luciferase activity (Turner Design)

Histone Acetyltransferase Assays—GST-NPAS2 was incubated with recombinant FLAG tagged p300 or CBP, and beads were washed extensively. Histone acetyltransferase (HAT) assays were performed on the beads using commercially available purified histones (Roche Applied Science) in the presence of ^{14}[C]acetyl-CoA (32) and run on 12% SDS gels. Acetylated histone H3 and histone H4 were analyzed by phosphorimager.

Transfection Studies—NIH3T3 cells were transiently transfected as described (31) with the E-box reporter construct pGL3M34Luc, pRLSV40 along with combinations of NPAS2, BMAL1, CLOCK, p300, CBP, PCAF, INHAT, E1A, TWIST, and CRY2 where indicated. The amount of DNA in each transfection was kept constant by addition of empty pCDNA3 vector. Cells were harvested 48 h post-transfection and assayed for luciferase activity by luminometer (Turner Design)

Immunofluorescence—Quiescent HVSMC were fixed in 4% paraformaldehyde in 0.1 M phosphate buffer and permeabilized by 0.2% Triton X in 0.1 M phosphate buffer. Cells were incubated with CLOCK or NPAS2 antibodies (Alpha Diagnostic and Affinity Bioreagents) and p300 (Upstate Biotechnology) antibodies and were incubated with a corresponding fluorescein isothiocyanate and Cy3-conjugated secondary antibody, following repeated washing. Cells were again washed and mounted on cover slips, and fluorescence was detected by confocal laser microscopy.

Co-immunoprecipitation Assays—Intact HeLa cells were incubated with the cross-linker DSP (Pierce Biotechnology) 3 mM for 30 min and lysed in buffer A (150 mM NaCl, 1 mM EDTA, 20 mM Tris-HCl, pH 8.0, 10% glycerol, and a mixture of protease inhibitors) for 2 h at 4 °C. Immunoprecipitations were carried out as described (31) with equal concentrations of protein and probed with anti-p300, anti-CBP (Upstate), and anti-PCAF (Santa Cruz Biotechnology) antibodies. Frozen whole mouse hearts were pulverized and protein extracted using lysis buffer A. Immunoprecipitations were carried out as detailed above.

RESULTS

Rhythmic Changes in Chromatin Remodeling on the Per1 Promoter—The *hPer1* gene contains 5 consensus E-box sequences (CACGTG), the strict consensus motif for heterodimeric bHLH-PAS CLOCK:BMAL1 binding. These occur within 4 kb of the *hPer1* gene promoter and each of which has been shown to contribute to the regulation of *Per1* expression (33). In contrast, the *hPer2* gene does not contain any such sequences within 1.6 kb of the promoter (34). Changes in mRNA levels of *hPer1* and *hPer2* in HeLa cells following serum induction were observed to exhibit a circadian expression pattern. *Per1* levels reached a trough at T6 and then entered a cyclical expression pattern, peaking at T24 and at T48. *Per2* levels, by contrast, remained high at T6, reached a measured trough at T12 exhibiting further peaks at approximately T18 and T42 (Fig. 1*A*). ChIP assays were performed on serum induced HeLa cells using primers that bracket the second most proximal E-box to exon 1 in the *hPer1* promoter (Fig. 1*B*). Histone H3 acetylation peaked at T42, while histone H4 acetylation peaked at T24 and T48 which coincides with the peaks of *hPer1* mRNA expression. Although we did not observe a peak in histone H3 acetylation in the first 24 h post-serum induction, the peak of histone H3 acetylation at T42 precedes that of maximum mRNA expression of hPer1 at T48. This is in agreement with our *in vivo* results (see below).

A sharp increase in unphosphorylated Pol II recruitment was also observed at T24 (Fig. 1*B*). These results are consistent with the temporal recruitment of enzymes with HAT activity to the promoter of clock-controlled genes activating circadian gene expression.

In Vitro Association of Core Clock Proteins and HAT Coactivator Proteins—Other members of the bHLH-PAS family interact with coactivator proteins, such as p300/CBP (35, 36). This prompted investigation of whether p300/CBP, PCAF, or

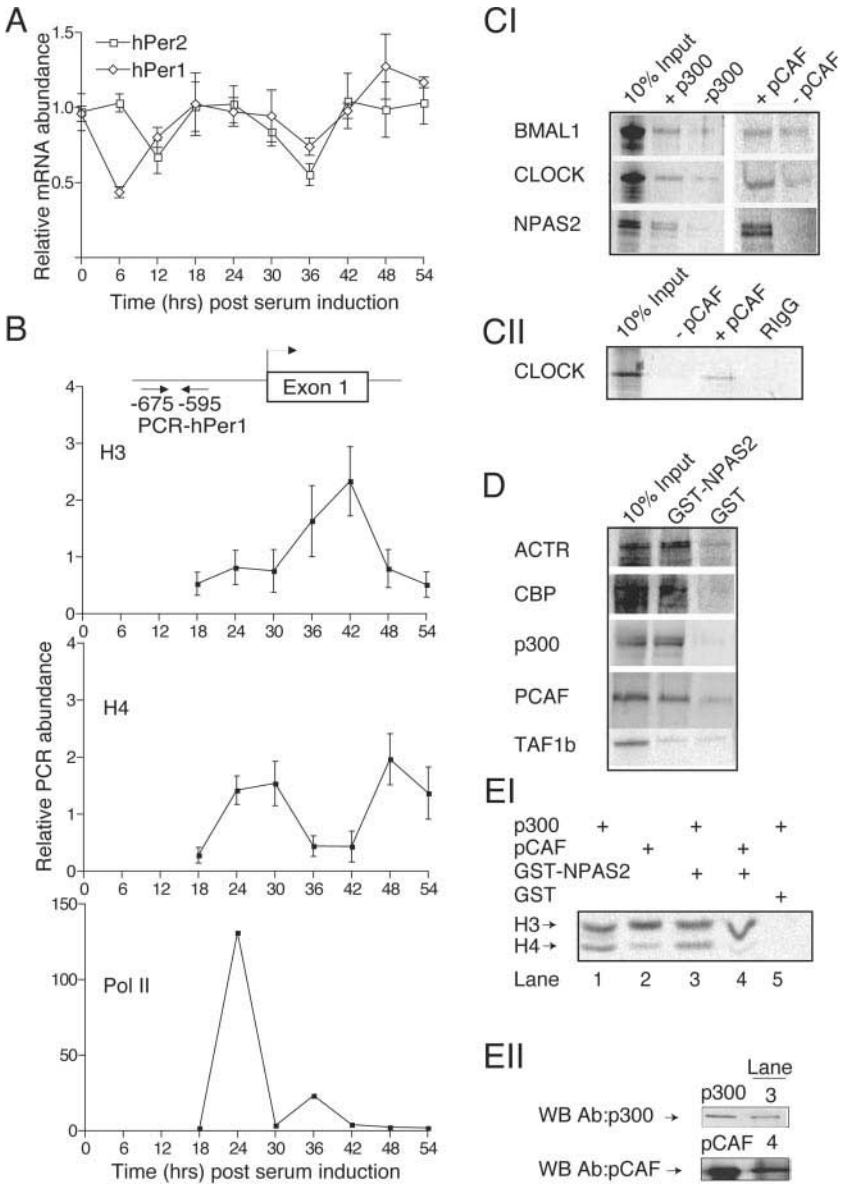

FIG. 1. **Chromatin remodeling on *hPer1* promoter and associated co-activator proteins.** *A*, quantitative analysis by real time PCR of *hPer1* and *hPer2* RNA expression in serum-induced HeLa cells. Each value is normalized to β-actin and expressed relative to the mean of each experiment. Values are mean ± S.E., $n = 3$. *B*, rhythm in histone H3 and histone H4 and Pol II recruitment on the second proximal E-box in the *hPer1* promoter. Serum-induced HeLa cells were harvested at 6-h intervals post-induction, and samples were subjected to X-ChIP using anti-acetyl histone H3, anti-acetyl histone H4, and N-terminal RNA Pol II antibodies. Histone H3 and histone H4 values are mean ± S.E., $n = 3$, unphosphorylated Pol II values, $n = 1$. *C*, *in vitro* co-immunoprecipitation of Clock proteins with recombinant p300 and PCAF. *D*, GST-NPAS2 pull-down assays with labeled ACTR, CBP, p300, PCAF, and TAF1β. *E*, p300 or PCAF complexed to NPAS2 still retains functional HAT activity (*panel I*). GST-NPAS2 complex from *lanes 3* and *4* (*panel I*) were probed using anti-p300 and anti-PCAF antibodies (*panel II*).

ACTR could interact specifically with CLOCK, BMAL1, or NPAS2. A modest interaction was observed between all three bHLH-PAS proteins and p300 (Fig. 1*C*, *panel I*), while PCAF was observed to associate preferentially with NPAS2 and, to a lesser extent, with CLOCK (Fig. 1*C*, *panel I*). Co-immunoprecipitation with anti-rabbit IgG in the presence of CLOCK and PCAF was used as an additional control (Fig. 1*C*, *panel II*). Importantly, and in agreement with the *in vitro* immunoprecipitation experiments, *in vitro* binding assays showed formation of complexes between ACTR, p300/CBP, and PCAF and the GST-NPAS2 glutathione-Sepharose affinity matrices, (Fig. 1*D*). This interaction was specific since a complex was not formed between GST-NPAS2 and TAFIβ, one of the subunits of the INHAT complex (31). Furthermore, both p300 and PCAF bound to GST-NPAS2 still retained functional HAT activity, as detected by acetylated histone H3 and histone H4. This activity is comparable to that of unbound p300 or PCAF (Fig. 1*E*, *panel I*). The identity of p300 or PCAF bound to GST NPAS2 was also verified by Western blotting (Fig. 1*E*, *panel II*).

Interaction of CLOCK Proteins with Coactivators in Intact Cells—The temporal colocalization of the endogenous proteins in primary cultures of human vascular smooth cells (HVSMC) was subsequently investigated. Immunofluorescent analysis of HVSMC by confocal microscopy revealed that CLOCK and p300 both exhibit predominantly nuclear localization, while NPAS2 is evident both in the nucleus and in the perinuclear cytoplasm in untreated quiescent cells (Fig. 2*A*). Overlay analysis of HVSMC immunostained with either anti-CLOCK or anti-NPAS2, together with anti-p300, produced discrete speckles of colocalization within the nucleus. This was more apparent for NPAS2 and p300 than for CLOCK and p300 (Fig. 2*A*). In addition, a Gal4BD fusion of NPAS2 and a VP16 fusion of CBP used in mammalian two-hybrid assays confirmed their association in intact cells, consistent with the GST pull-down experiments (Fig. 2*B*). The association of endogenous coactivators to clock proteins was then investigated in intact cells. CLOCK and NPAS2, immunoprecipitated from quiescent HeLa cell lysates, were probed for the presence of the coactivator p300, CBP, and PCAF. p300 co-precipitated with CLOCK and, to a lesser extent, NPAS2 (Fig. 2*C*). However, CBP was only detected from immunoprecipitated CLOCK and not NPAS2 (Fig. 2*C*). Interestingly, PCAF selectively coprecipitated with only NPAS2 in these cells (Fig. 2*C*).

Given the precedent with CLOCK and p300 in the liver (27), we hypothesized that the NPAS:p300 interaction might exhibit temporal regulation. HeLa cells were serum shocked and ly-

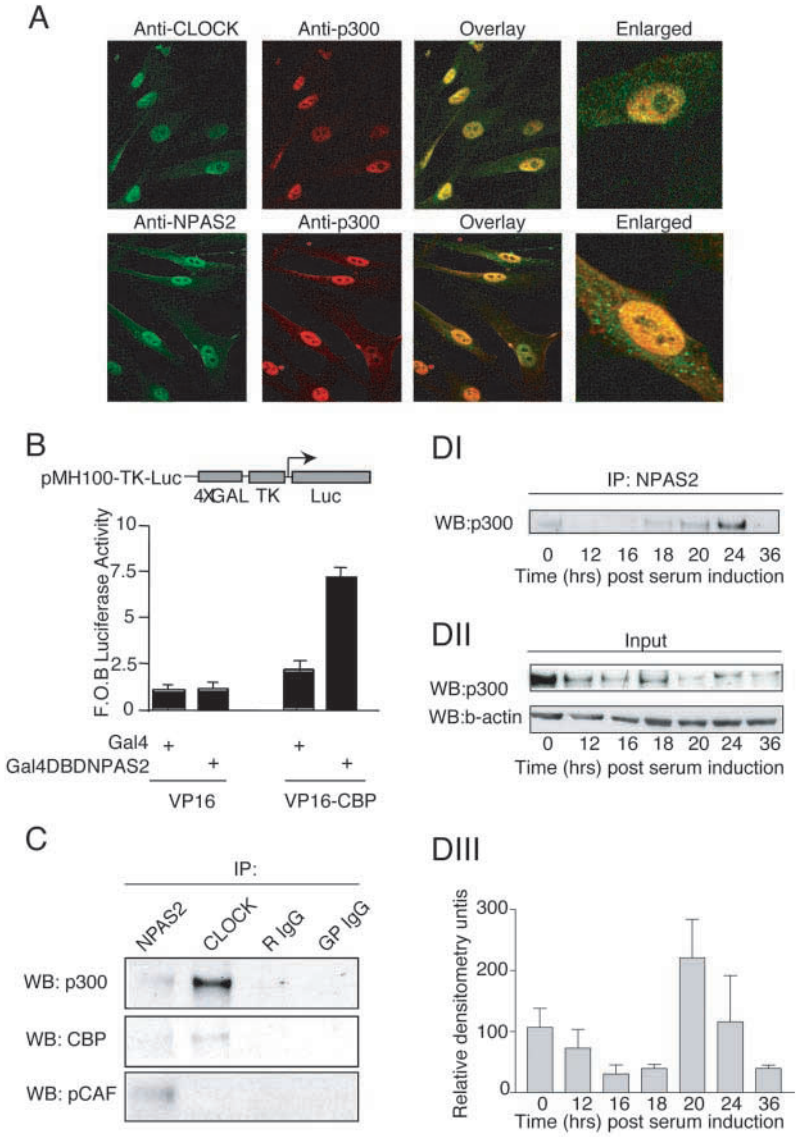

FIG. 2. **Interaction of Clock proteins with co-activators *in vitro* and in intact cells.** *A*, p300, NPAS2, and CLOCK colocalize in the nuclear regions of HVSMCs. Resting hVSMCs were incubated with anti-CLOCK or NPAS2 and p300. Fluorescence was detected by confocal laser microscopy (*B*) CBP interacts with NPAS2 in intact cells by mammalian two-hybrid assay. CV-1 cells were transiently transfected with the reporter construct pMH100-TKLuc and various DNAs as indicated. Cells were harvested 48-h post-transfection and assayed for luciferase activity. *F.O.B*, Fold Over Basal. *C*, co-precipitation of coactivators with clock proteins in HeLa cells. Lysates from quiescent HeLa cells was split in equal parts and immunoprecipitated (*IP*) with antibodies against CLOCK and NPAS2 and rabbit and guinea pig IgG as controls. Immunocomplexes were probed for p300, CBP, and PCAF. *D*, NPAS2 displays a time-dependent association with p300 in serum-induced HeLa cells. Representative blot of a single time course experiment (*panel I*). Representative expression of input p300 and β-actin in serum induced cells (*panel II*). Quantitative analysis of p300:NPAS2 interaction (*panel III*). p300 bands were quantified using densitometry methods and normalized using β-actin values. Data are mean values $\pm$ S.E., $n = 3$.

sates taken at intervals following treatment. They were immunoprecipitated with NPAS2 and the immune complexes were probed for p300. Though only a modest association between NPAS2 and p300 was observed in quiescent cells (Fig. 2*C*), a robust and dynamic interaction occurred in synchronized cells (Fig. 2*D*, *panel I*). The interaction between NPAS2 and p300 decreased at T16 and T18 compared with T0 (Fig. 2*D*, *panel III*). This trough was followed by a significant increase, at T20 and T24, which corresponded with maximum RNA levels of *Per1* and *Per2* (Fig. 1*A*). A low level of interaction was again evident at T36, synchronous with a fall in Per1 and Per2 mRNA levels (Fig. 2*D*, *panel III*). All data was normalized to β-actin (Fig. 2*D*, *panel II*). The observation that serum-induced cells display a rhythm in histone acetylation surrounding the *Per1* promoter and that NPAS2 associates in a time-dependent manner with histone acetyltransferases at a time of maximum transcriptional activity is consistent with regulation of the circadian feedback loop.

Transcriptional Activity of NPAS2/CLOCK:BMAL1 Is Modulated by Acetylation—The association of the clock bHLH-PAS proteins with the HATs, p300/CBP, PCAF and ACTR, is consistent with a role for targeted coactivator recruitment and chromatin remodeling in the temporal regulation of circadian gene activation in the mammalian feedback loop. This hypothesis was addressed by analyzing the effect of overexpression of the HAT-coactivators on E-box-induced gene transcription in intact cells. Both NPAS2:BMAL1 and CLOCK:BMAL1 activated transcription via an E-box-dependent mechanism (10). Importantly, and consistent with previous interaction specificity assays, over expression of CBP and PCAF markedly enhanced NPAS2- and CLOCK-mediated luciferase reporter gene activation (Fig. 3, *A* and *B*). In addition, coactivation of E-box-dependent transcription was maximally enhanced when CBP and PCAF were co-expressed (Fig. 3, *A* and *B*). Cotransfection of deletion mutants of NPAS2, NPAS2Δ322 and NPAS2Δ425, decreased the transactivation of BMAL1 by full-length NPAS2, indicating a direct effect of the coactivators on the transcription factor complex (Fig. 3*C*, *panel II*). Both of these mutants lack the L*XX*LL motif (Fig. 3*C*, *panel I*), which is present in nuclear receptor cofactors and in the ligand binding domains (LBDs) of some nuclear receptors, and is necessary for their interactions (37). Thus, both recruitment of specific coactivators to the clock complex and HAT-dependent activation are critical features of CLOCK/NPAS2:BMAL1-mediated E-box activation.

Furthermore, the histone acetylation regulatory proteins, E1A and Twist (32, 38) and the histone masking complex

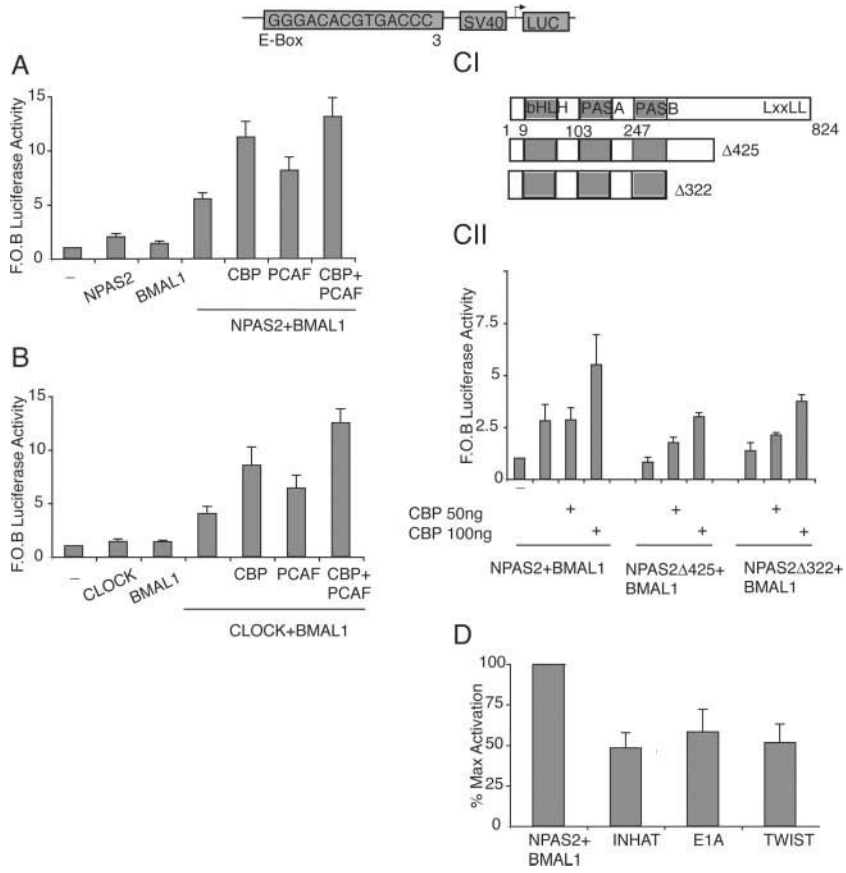

FIG. 3. **Transcriptional activity of NPAS2/CLOCK:BMAL1 is modulated by acetylation and deacetylation.** *A*, E-box-dependent activation by NPAS2: BMAL1 and *B*, CLOCK:BMAL1 is markedly enhanced in the presence of CBP and PCAF. *F.O.B*, Fold Over Basal. NIH3T3 cells were transiently transfected with the E-box reporter construct pGL3M34-Luc (100 ng), along with pRLSV40 (5 ng) and CMX constructs of CLOCK/NPAS2: BMAL1 (50 ng) with or without CBP or PCAF (200 ng). *C*, representation of the regions of NPAS2, which correspond to the deletion mutants (*panel I*). NPAS2 deletion mutants lacking the L*XX*LL motif show a reduction in transcriptional activity in the presence of increasing amounts of CBP (*panel II*). *D*, histone acetylation regulatory proteins E1A and Twist, and the histone masking complex, INHAT, can all repress basal E-box-mediated activation of NPAS2:BMAL1. NIH3T3 cells were transfected as described in *A* with CMX constructs of NPAS2:BMAL1 along with the three subunits of the INHAT complex: Set/TAF-Iβ, TAF-Iα, and pp32 (50 ng each), E1A (10 ng) and TWIST (50 ng). For all figures, each value is the mean of at least two independent experiments ± S.E. Each experiment included six replicates from a single assay.

INHAT (31), can all repress basal E-box activation of NPAS2: BMAL1 (Fig. 3*D*), providing further evidence for underlying HAT-dependent regulation of these circadian transcriptional co-regulators.

Analyses of Chromatin Remodeling and Coactivator Recruitment in Vivo—Real time PCR was used to examine mRNA expression profiles of *Npas2*, *Bmal1*, *Clock*, *Per (1–2)*, *Cry1*, and *Rev-erb*α within cardiac tissue. This was obtained from Balb/c mice, which had been maintained in constant darkness. Hearts were harvested at 4-h intervals, over a 48-h period (Fig. 4*A*). *Npas2* and *Bmal1* cycled in the same phase, peaking at approximately ct1 and again at approximately ct29 (Fig. 4*A*, *panel I*). *Clock* expression does not cycle robustly throughout the daily period (Fig. 4*A*, *panel I*), as previously reported (9, 18). In addition, *Rev-erb*α mRNA oscillation was antiphase to that of *Bmal1* mRNA (Fig. 4*A*, *panel II*). This is in agreement with the finding that REV-ERBα can repress *Bmal1* expression through binding to the ROR response elements in the promoter of Bmal1 (16). Both *Per1* and *Per2* cycled rhythmically and in phase with each other, but antiphase to the genes, which drive their oscillatory expression, *Bmal1*, *Npas2*, and *Clock* (Fig. 4*A*, *panel III*).

ChIP assays were performed on whole mouse heart homogenates taken at ct 6, 18, and 32 and analyzed using primers that bracket the most proximal E-box to exon 1 in the *mPer1* promoter (Fig. 4*B*). Consistent with previous observations (27), time-dependent histone H3 acetylation, was observed on the proximal E-box, preceding the *Per1* rhythm (Fig. 4*A*, *panel III*). This is in agreement with the *in vitro* data from serum induced HeLa cells, where the peak in histone H3 acetylation at T42 preceded Per1 maximum expression at T48 (Fig. 1*B*).

Immunoprecipitations using anti-rabbit IgG was used to determine nonspecific interactions of NPAS2 in whole mouse heart homogenates (Fig. 4*C*, *panel I*). Anti-NPAS2 immunoprecipitates showed significant temporal changes in both association and disassociation of p300 bound to NPAS2 (Fig. 4*C*, *panel II*). Interestingly, association was increased at T6 and T32 correlating with the rise of *Per1* mRNA and the increase in histone H3 acetylation levels on the E-box surrounding its promoter (Fig. 4*A*, *panel III* and Fig. 4*B*). In addition to regulating *Per1*, CLOCK and BMAL1 have been shown also to drive rhythmically *Cry* expression (10, 15, 39). The observation that NPAS2-p300 association also increases at T20, preceding peak Cry expression (Fig. 4*A*, *panel II*), is consistent with a pervasive role for HAT-dependent mechanisms in regulating clock gene expression. Finally, using E-box reporter transactivation studies, we observe CRY2 mediated repression on basal NPAS2 and CLOCK-mediated luciferase reporter gene activation (Fig. 4*D*). Importantly, overexpression of CBP was partially able to relieve this repression, indicating that modulation of histone acetylation may be the target of CRY mediated E-box repression (Fig. 4*D*).

DISCUSSION

Acetylation of core histones on target promoters has been closely linked to transcriptional gene activation (22). In the present study, the coincidence of a rhythm in histone H3 and histone H4 acetylation on the proximal E-box of hPer1 with transcriptional activation of *per1* and *per2* is consistent with the heterodimeric complexes of CLOCK, NPAS2 and BMAL1 recruiting a histone acetyltransferase (HAT)-containing transcriptional co-activation complex to achieve maximal target gene activation. We considered p300, CBP, PCAF, and ACTR as potential circadian coactivators, all of which are known to possess acetyltransferase activity (40–42). Other known members of the bHLH-PAS family, such as HIF-1α and the AHR: AHRNT heterodimer, utilize p300/CBP to augment gene transcription (35, 36).

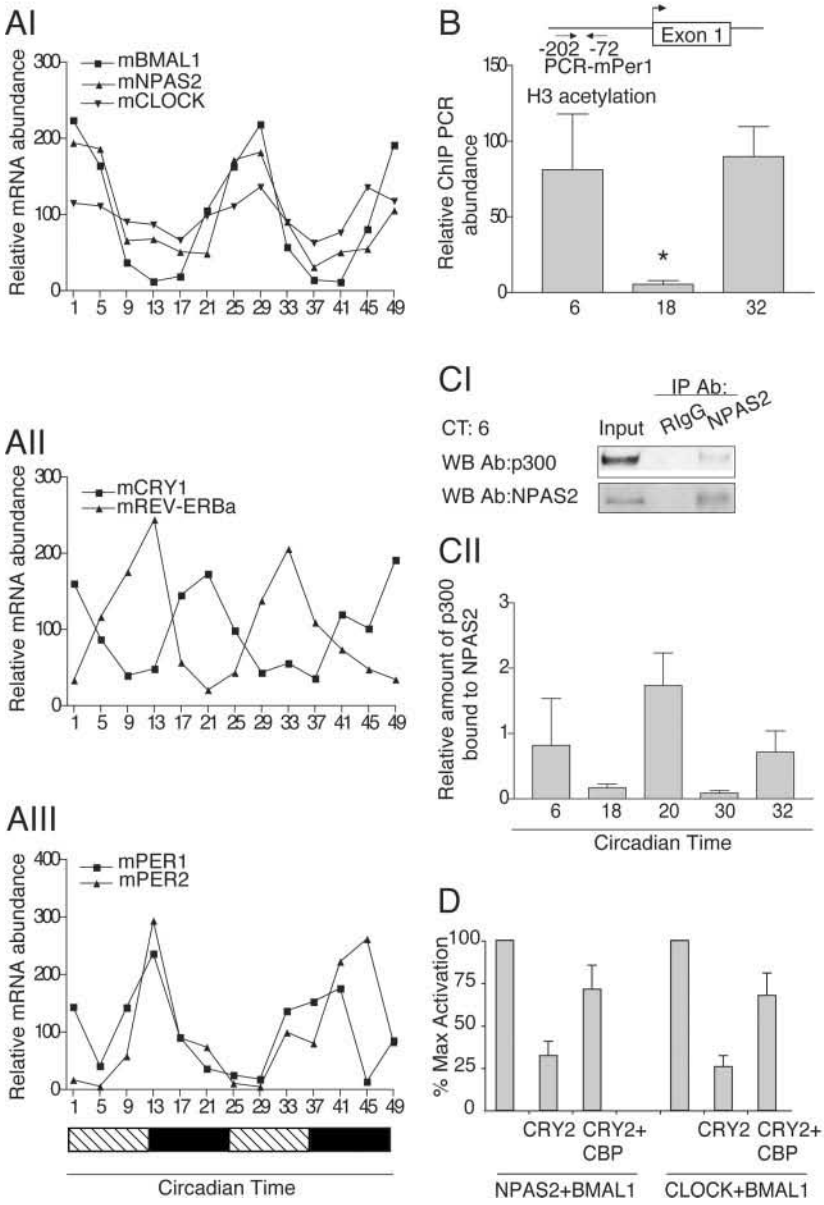

FIG. 4. **Analysis of chromatin remodeling and coactivator recruitment in heart.** *A*, mRNA expression profiles of clock genes in mouse heart tissue by Real time PCR. Each data point represents three pooled samples. *B*, temporal histone H3 acetylation on the *mPer1* promoter in mouse heart tissue. (Kruskal Wallis Statistic, 10.75; *, $p < 0.01$, ct 6 *versus* ct 18 $p < 0.05$, ct18 *versus* ct32 $p < 0.01$). The graph shows Real time PCR values; data are mean values ± S.E., $n = 3–6$. *C*, p300 associates with NPAS2 *in vivo*. Representative blot from ct 6 showing IP with anti-NPAS2 and control anti-RIgG (*panel I*). Quantification of p300 bound to NPAS2 at indicated time points (Kruskal Wallis Statistic, 12.79, $p < .05$). p300 bands were quantified by densitometry and standardized relative to amount of NPAS2 present. Data are mean values ± S.E. ($n = 3–5$). *D*, CRY2 inhibition of NPAS2:BMAL1 and CLOCK:BMAL1 E-box-dependent activity is rescued by overexpression of CBP.

We have demonstrated an interaction between both CLOCK and NPAS2 with p300, CBP, PCAF, and ACTR by *in vitro* interaction assays. Importantly, this interaction does not constrain the enzymatic activity of p300 and PCAF, allowing them freely to acetylate core histones. The interactions of CLOCK and NPAS2 with p300, CBP, and PCAF were also observed in resting cells. Indeed, the binding of CBP to CLOCK and of PCAF to NPAS2, raises the possibility of selective association of proteins to elements of the clock transcription complex in a manner which might relate to tissue type and/or activation stimulus. Thus, p300 interacts in a time-dependent manner with NPAS2 under synchronized conditions. Increased association was observed at the time of maximal RNA expression, suggesting that temporal coactivator recruitment is a necessary step in driving circadian rhythmicity. This association is dramatically reduced at T12 and T36 corresponding with Cry2 mediated repression of Per1 and Per2. This finding agrees with the model proposed by Etchegaray *et al.* (27) that Cry proteins may disrupt the Clock associated transcriptional coactivator complex.

Cell-based luciferase assays using an E-box reporter revealed that the transcriptional activity of CLOCK:BMAL1 and NPAS2:BMAL1 heterodimers is enhanced in the presence of CBP and PCAF and a further increase in activity occurs when CBP and PCAF are co-expressed together. CBP and PCAF are known to act cooperatively to enhance transcriptional activity of both FKLF2 (43) and IFN-β, the latter one of the best characterized transcriptional switches in eukaryotic cells (44). In the present studies, basal E-box activation was sensitive to inhibition by enzymes and complexes, which are known to inhibit or block HAT activity or function, highlighting the importance of HAT activity in regulating circadian gene expression.

A time-dependent recruitment of chromatin remodeling machinery by NPAS2 was also observed *in vivo*. Increased association of NPAS2 with p300 resulted in marked acetylation of N-terminal lysine residues on histone H3 surrounding the proximal E-box on the *Per1* promoter in mouse heart homogenates, which was synchronous with circadian variability in its mRNA levels. The mechanism by which the cryptochrome proteins potently inhibit CLOCK/NPAS2:BMAL1-mediated transcription is presently unclear (15). However, overexpression of CBP was partially able to relieve this repression, indicating that modulation of histone acetylation may be the target of CRY-mediated E-box repression (Fig. 4*D*).

Targeted histone acetylation surrounds the proximal E-boxes on the *Per1* promoter, causing localized chromatin remodeling and enhanced assembly of the basal transcription machinery. This regulates circadian gene expression in the cardiovascular system. Periodic recruitment of p300 to NPAS2 facilitates time-dependent chromatin remodeling and CRY2-mediated repression is induced by disruption of HAT-associated complexes on core clock heterodimers. These studies provide insight into the regulation of circadian rhythms in the cardiovascular system and elucidate further the fundamental role of chromatin remodeling in mammalian circadian biology.

Acknowledgments—We thank Tilo Grosser, Amita Sehgal, and J. D. Alverez for their helpful suggestions. We appreciate all the technical assistance provided by E. V. Kostetskaia and Emma Sankoorikal. We also thank Drs. C. Bradfield and J. Hogenesch for NPAS2/MOP4, CLOCK, and BMAL1/MOP3 cDNA clones and the M34-Luc reporter vector, and Dr. S. McKnight for the NPAS2/MOP4 cDNA clone. We also thank Dr. S. Reppert for the generous gift of the CLOCK antibody.

REFERENCES

1. Panda, S., Hogenesch, J. B., and Kay, S. A. (2002) *Nature* **417,** 329–335
2. Reppert, S. M., and Weaver, D. R. (2001) *Annu. Rev. Physiol.* **63,** 647–676
3. Ralph, M. R., Foster, R. G., Davis, F. C., and Menaker, M. (1990) *Science* **247,** 975–978
4. Cheng, M. Y., Bullock, C. M., Li, C., Lee, A. G., Bermak, J. C., Belluzzi, J., Weaver, D. R., Leslie, F. M., and Zhou, Q. Y. (2002) *Nature* **417,** 405–410
5. Kramer, A., Yang, F. C., Snodgrass, P., Li, X., Scammell, T. E., Davis, F. C., and Weitz, C. J. (2001) *Science* **294,** 2511–2515
6. Balsalobre, A., Brown, S. A., Marcacci, L., Tronche, F., Kellendonk, C., Reichardt, H. M., Schutz, G., and Schibler, U. (2000) *Science* **289,** 2344–2347
7. Le Minh, N., Damiola, F., Tronche, F., Schutz, G., and Schibler, U. (2001) *EMBO J.* **20,** 7128–7136
8. McNamara, P., Seo, S. B., Rudic, R. D., Sehgal, A., Chakravarti, D., and FitzGerald, G. A. (2001) *Cell* **105,** 877–889
9. Shearman, L. P., Sriram, S., Weaver, D. R., Maywood, E. S., Chaves, I., Zheng, B., Kume, K., Lee, C. C., van der Horst, G. T., Hastings, M. H., and Reppert, S. M. (2000) *Science* **288,** 1013–1019
10. Gekakis, N., Staknis, D., Nguyen, H. B., Davis, F. C., Wilsbacher, L. D., King, D. P., Takahashi, J. S., and Weitz, C. J. (1998) *Science* **280,** 1564–1569
11. Hogenesch, J. B., Chan, W. K., Jackiw, V. H., Brown, R. C., Gu, Y. Z., Pray-Grant, M., Perdew, G. H., and Bradfield, C. A. (1997) *J. Biol. Chem.* **272,** 8581–8593
12. Hogenesch, J. B., Gu, Y. Z., Jain, S., and Bradfield, C. A. (1998) *Proc. Natl. Acad. Sci. U. S. A.* **95,** 5474–5479
13. Reick, M., Garcia, J. A., Dudley, C., and McKnight, S. L. (2001) *Science* **5,** 5
14. Dudley, C. A., Erbel-Sieler, C., Estill, S. J., Reick, M., Franken, P., Pitts, S., and McKnight, S. L. (2003) *Science* **301,** 379–383
15. Kume, K., Zylka, M. J., Sriram, S., Shearman, L. P., Weaver, D. R., Jin, X., Maywood, E. S., Hastings, M. H., and Reppert, S. M. (1999) *Cell* **98,** 193–205
16. Nicolas Preitner, F. D., Luis-Lopez-Molina, Joszef Zakany, Denis Duboule, Urs Albrecht, and Ueli Schibler. (2002) *Cell* **110,** 251–260
17. Eide, E. J., Vielhaber, E. L., Hinz, W. A., and Virshup, D. M. (2002) *J. Biol. Chem.* **277,** 17248–17254
18. Lee, C., Etchegaray, J. P., Cagampang, F. R., Loudon, A. S., and Reppert, S. M. (2001) *Cell* **107,** 855–867
19. Kondratov, R. V., Chernov, M. V., Kondratova, A. A., Gorbacheva, V. Y., Gudkov, A. V., and Antoch, M. P. (2003) *Genes Dev.* **17,** 1921–1932
20. Strahl, B. D., and Allis, C. D. (2000) *Nature* **403,** 41–45
21. Grunstein, M. (1997) *Nature* **389,** 349–352
22. Brownell, J. E., and Allis, C. D. (1996) *Curr. Opin. Genet. Dev.* **6,** 176–184
23. Nakajima, T., Uchida, C., Anderson, S. F., Lee, C. G., Hurwitz, J., Parvin, J. D., and Montminy, M. (1997) *Cell* **90,** 1107–1112
24. Agalioti, T., Lomvardas, S., Parekh, B., Yie, J., Maniatis, T., and Thanos, D. (2000) *Cell* **103,** 667–678
25. Yie, J., Senger, K., and Thanos, D. (1999) *Proc. Natl. Acad. Sci. U. S. A.* **96,** 13108–13113
26. Crosio, C., Cermakian, N., Allis, C. D., and Sassone-Corsi, P. (2000) *Nat. Neurosci.* **3,** 1241–1247
27. Etchegaray, J. P., Lee, C., Wade, P. A., and Reppert, S. M. (2003) *Nature* **421,** 177–182
28. Kel, A. E., Kel-Margoulis, O. V., Farnham, P. J., Bartley, S. M., Wingender, E., and Zhang, M. Q. (2001) *J. Mol. Biol.* **309,** 99–120
29. Weinmann, A. S., Bartley, S. M., Zhang, T., Zhang, M. Q., and Farnham, P. J. (2001) *Mol. Cell. Biol.* **21,** 6820–6832
30. Wells, J., Boyd, K. E., Fry, C. J., Bartley, S. M., and Farnham, P. J. (2000) *Mol. Cell. Biol.* **20,** 5797–5807
31. Seo, S. B., McNamara, P., Heo, S., Turner, A., Lane, W. S., and Chakravarti, D. (2001) *Cell* **104,** 119–130
32. Chakravarti, D., Ogryzko, V., Kao, H. Y., Nash, A., Chen, H., Nakatani, Y., and Evans, R. M. (1999) *Cell* **96,** 393–403
33. Hida, A., Koike, N., Hirose, M., Hattori, M., Sakaki, Y., and Tei, H. (2000) *Genomics* **65,** 224–233
34. Travnickova-Bendova, Z., Cermakian, N., Reppert, S. M., and Sassone-Corsi, P. (2002) *Proc. Natl. Acad. Sci. U. S. A.* **99,** 7728–7733
35. Kallio, P. J., Okamoto, K., O'Brien, S., Carrero, P., Makino, Y., Tanaka, H., and Poellinger, L. (1998) *EMBO J.* **17,** 6573–6586
36. Kobayashi, A., Numayama-Tsuruta, K., Sogawa, K., and Fujii-Kuriyama, Y. (1997) *J. Biochem.* (*Tokyo*) **122,** 703–710
37. Glass, C. K., and Rosenfeld, M. G. (2000) *Genes Dev.* **14,** 121–141
38. Hamamori, Y., Sartorelli, V., Ogryzko, V., Puri, P. L., Wu, H. Y., Wang, J. Y., Nakatani, Y., and Kedes, L. (1999) *Cell* **96,** 405–413
39. Jin, X., Shearman, L. P., Weaver, D. R., Zylka, M. J., de Vries, G. J., and Reppert, S. M. (1999) *Cell* **96,** 57–68
40. Ogryzko, V. V., Schiltz, R. L., Russanova, V., Howard, B. H., and Nakatani, Y. (1996) *Cell* **87,** 953–959
41. Yang, X. J., Ogryzko, V. V., Nishikawa, J., Howard, B. H., and Nakatani, Y. (1996) *Nature* **382,** 319–324
42. Chen, H., Lin, R. J., Schiltz, R. L., Chakravarti, D., Nash, A., Nagy, L., Privalsky, M. L., Nakatani, Y., and Evans, R. M. (1997) *Cell* **90,** 569–580
43. Song, C. Z., Keller, K., Murata, K., Asano, H., and Stamatoyannopoulos, G. (2002) *J. Biol. Chem.* **277,** 7029–7036
44. Munshi, N., Agalioti, T., Lomvardas, S., Merika, M., Chen, G., and Thanos, D. (2001) *Science* **293,** 1133–1136